Available online at www.sciencedirect.com
SCIENCE DIRECT®
Experimental Thermal and Fluid Science 28 (2004) 701–708
Experimental Thermal and Fluid Science
www.elsevier.com/locate/etfs

# Reference components of jet fuels: kinetic modeling and experimental results

A. Agosta [a], N.P. Cernansky [a], D.L. Miller [a], T. Faravelli [b], E. Ranzi [b,*]

[a] Department of Mechanical Engineering and Mechanics, Drexel University, USA
[b] CMIC Department, Politecnico di Milano, Piazza Leonardo da Vinci 32, Milan 20133, Italy

Received 20 June 2003; received in revised form 15 November 2003; accepted 1 December 2003

**Abstract**

The goal of this work is to give some kinetic insight on the autoignition and combustion behaviour of full boiling range hydrocarbon fuels. The initial attention is devoted to the selection of possible components of a surrogate that reproduces the reaction behaviour of typical real fuels. *n*-Dodecane and iso-cetane are the reference components for the different alkane classes, while methylcyclohexane and decalin represented naphthenes and alphamethylnaphthalene represented aromatics. Several oxidation results have been obtained in a pressurized flow reactor both for neat components and selected mixtures. The reactivity maps of the different experiments are reported in terms of CO production. The experimental results clearly confirm that autoignition properties of the mixture cannot be simply reproduced by linear blending rules. Semi-detailed or lumped kinetic models for the oxidation and combustion of pure components are briefly discussed and model predictions are compared with the overall set of experimental measurements. The general agreement with the experimental data, including the mixtures, indicates the viability and interest of the proposed approach.


*Keywords:* Detailed kinetics; Surrogate fuels; Combustion

## 1. Introduction

The next generation of civilian and military vehicles will demand higher performance propulsion systems that deliver increased power and fuel efficiency, while producing lower observable emissions. There is strong evidence that low and intermediate temperature hydrocarbon fuel chemistry controls the important preignition processes through heat release and formation of reactive species [1–3]. The elucidation of the hydrocarbon chemistry during these phases of operations remains an important goal of combustion as it applies to engine and propulsion systems. This study is an effort to expand the actual knowledge of the autoignition behavior of single and multi-component mixtures of full boiling range distillate hydrocarbon fuels, chosen as representative components of diesel and jet fuels.

As a rule, there are large temperature gradients in combustion devices during operation, and the fuel can spend considerable time in one or both of the low and intermediate temperature regimes. Thus, the oxidation chemistry in the lower temperature regimes can have a significant role in the overall combustion process, in some cases accounting for substantial heat release and grossly changing the input conditions to the high temperature zone. Further, combustion devices in common use within the transportation sector (diesel, spark ignition, and gas turbine engines) operate exclusively at elevated pressures. Consequently, fundamental research on low and intermediate temperature oxidation chemistry and at pressures above one atmosphere is important to understanding many practical combustion phenomena including: cold-start, preignition fuel decomposition, pollutant formation, and general autoignition processes.

Over the years, a considerable amount of research has addressed the chemistry of the small hydrocarbons [4], particularly in the cool flame and two-stage ignition

* Corresponding author. Tel.: +39-02-23-99-32-50; fax: +39-02-23-99-32-50/70-63-81-73.
*E-mail address:* eliseo.ranzi@polimi.it (E. Ranzi).

0894-1777/$ - see front matter © 2004 Elsevier Inc. All rights reserved.
doi:10.1016/j.expthermflusci.2003.12.006

regions. Typical studies in the low and intermediate temperature regions were conducted using the gasoline reference fuels, *n*-heptane and iso-octane, and their blends. As noted by Edwards [5], the fundamental combustion behavior of the high-order hydrocarbons, mainly compounds with more than 8 carbon atoms, has received comparatively little study. Only recently did studies start examining larger hydrocarbons [6,7], but are still limited in scope and focused on a few major components of distillate fuels. Moreover, since complexity increases with the number of constituents, only a few studies have focused on the combustion aspects of complex mixtures of hydrocarbons.

Our initial attention was devoted to the selection of possible reference components in order to experimentally reproduce the interesting properties of real distillate fuels, such as the widely used JP-8 aviation fuel or other diesel and aviation fuels. These fuels are mixtures of several hundred different compounds, whose individual volumetric concentrations are often lower than 1% and, most of all, vary significantly from batch to batch, depending upon several factors including the parent crude oil used and the refinery processes involved.

First considering the alkanes group, which is the prevalent functional group in distillate fuels (i.e. alkanes represent approximately 60% of JP-8 entire volume), two components have been selected: a normal alkane, *n*-dodecane, and a branched alkane, isocetane (2,2,4,4,6,8,8-heptamethyl-nonane), the low-end reference fuel for the Cetane number rating scale. While it is still debated whether the approximation of the alkane portion of JP-8 would be better with a normal or a branched alkane [8], our previous research showed the fundamental importance of both structures and therefore both hydrocarbon types have been investigated [9].

Aromatic hydrocarbons are also major constituents of distillate fuels (i.e. typically aromatics comprise 20% of JP-8). The selected aromatic hydrocarbon is the bicyclic compound α-methylnaphthalene, the former low end reference compound of the cetane scale.

Cycloalkanes, also known as naphthenes, are the last major functional group in aviation fuels. Naphthenes are always present in distillate fuels and an in-depth knowledge of their combustion properties is of great interest for several reasons. First of all, naphthenes are characterized by an enhanced energy and volumetric density, and a lowered fuel freeze point useful to reach higher altitude operability. As an example, the Russian T-6 jet fuel is a typical higher-density, naphthenic jet fuel. Further, remaining in the aviation fuels field, possible future propellants examined by the USAF include the naphthenes-rich coal-derived fuels. These fuels are similar to JP-8X, a high-density version of JP-8, and are characterized by a 50% volumetric content of naphthenes, as compared to the 20% in conventional JP-8 [10]. Moreover, the attention recently being paid to homogeneous charge compression ignition (HCCI) as a clean alternative to the SI engine, has contributed to the actual request of a deeper understanding of the combustion characteristics of liquid fuels in general, and naphthenes in particular [11]. In this study, cycloalkanes have been represented by the monocyclic compound, methylcyclohexane, and the bicyclic compound, decalin.

This is not the only study to investigate and propose surrogates for heavy distillate fuels such as JP-8. Fig. 1 shows a comparison of the surrogate developed in this study along with two other proposed surrogates. Each of these surrogates was developed to map a selected set

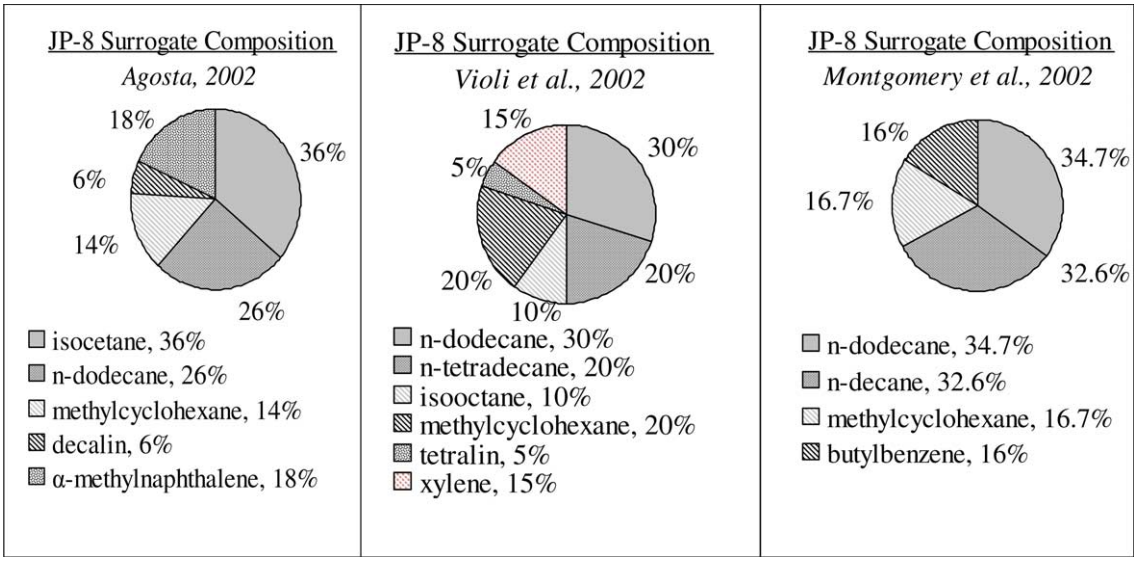


Fig. 1. Composition of representative JP-8 surrogates.

of physical, chemical, and reaction parameters. Discussions are underway to coordinate these efforts to determine what might be necessary to develop a universal JP-8 surrogate.

## 2. Experimental methodology

The experiments to investigate the oxidation chemistry of neat distillate hydrocarbons and their mixtures were carried out in the Drexel pressurized flow reactor (PFR) facility over a range of pressures (up to 12 atm) and temperatures in the interval 600–900 K. The pressurized flow reactor used in this study is similar to that described earlier [12]. The PFR has a temperature range up to 1000 K, which is effective to characterize the low and intermediate temperature regimes, and it is maintained at nearly adiabatic conditions so that the heat transfer effects can be ignored. In the PFR, a stream of pre-vaporized fuel is diluted using nitrogen and, as it enters the adiabatic quartz reaction duct, it is mixed into a stream of oxygen diluted with nitrogen. Fuel and oxygen concentrations are selected to slow the chemistry and to match the reaction time available in the PFR. During each experiment, samples of the reacting gases are withdrawn from the reactor centerline at varying axial locations with a glass-lined, water-cooled gas-sampling probe. Extracted gases are continuously directed to a NDIR gas analyzer for CO and $CO_2$ concentration measurements.

In order to observe the oxidation behavior of the selected hydrocarbons and mixtures, controlled cool down (CCD) experiments were carried out. In these experiments the reactor is stabilized at a specified $T_{max}$ (~900 K) and then allowed to cool at a fixed rate (~5 °C/min). CO is measured and recorded as a function of probe temperature to obtain a map of the reactivity over a range of temperatures (typically 900–600 K). As the reaction time is on the order of 150 ms and the cool down rate is 5 °C/min each datum represents a quasi-isothermal experiment at the temperature of the reactor. To achieve this constant reaction time the probe is moved by computer control toward the injector as the temperature decreases. The validity and success of the CCD methodology has been proved elsewhere [13] and is acceptable mainly because the oxidation reactions dominant in both the low and the NTC temperature regions quickly produce CO and CO is not converted to $CO_2$ at a significant rate (typical CO and $CO_2$ profiles are shown in Fig. 2, where the range of a generic CCD experiment is highlighted).

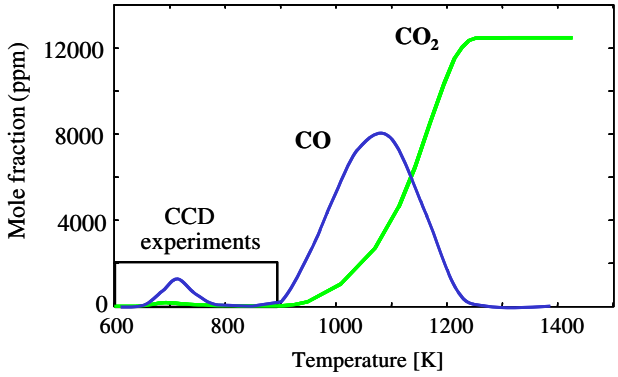


Fig. 2. CO and $CO_2$ production vs. reactor temperature for *n*-dodecane oxidation (ND1), showing the typical extent of a CCD experiment.

In an effort to expand kinetic and mechanistic information for large hydrocarbon oxidation, an initial set of experiments examined the oxidation characteristics of the following pure hydrocarbons: *n*-dodecane, isocetane, methylcyclohexane, and α-methylnaphthalene. The experimental conditions for the CCD experiments with these fuels and their binary mixtures are reported in Table 1. Clear and strong NTC behavior has been directly observed for pure *n*-dodecane, while the isocetane

Table 1
Summary of experimental conditions

| Exp. # | Fuel | | Φ | P [atm] | Res. time [ms] | Fuel molar fraction [ppm] |
|---|---|---|---|---|---|---|
| ND-1 | *n*-Dodecane | | 0.20 | 8 | 120 | 454 |
| ND-2 | *n*-Dodecane | | 0.25 | 8 | 120 | 567 |
| ND-3 | *n*-Dodecane | | 0.30 | 8 | 120 | 680 |
| IC-1 | Iso-cetane | | 0.70 | 8 | 180 | 2906 |
| MC-1 | Methylcyclohexane | | 0.30 | 8 | 120 | 1199 |
| MC-2 | Methylcyclohexane | | 0.40 | 8 | 120 | 1598 |
| MN-1 | α-Methylnaphthalene | | 0.30 | 8 | 175 | 1398 |
| MN-2 | α-Methylnaphthalene | | 0.70 | 12 | 250 | 3798 |
| M1-1 | Mix. M1 | 40% *n*-C12 | 0.30 | 8 | 120 | 870 |
| M1-2 | | 60%iso-C16 | 0.30 | 8 | 120 | 580 |
| M2-1 | Mix. M2 | 37% *n*-C12 | 0.30 | 8 | 120 | 1516 |
| M2-2 | | 63% MCH | 0.30 | 8 | 120 | 1011 |
| M3-1 | Mix. M3 | 51% *n*-C12 | 0.30 | 8 | 120 | 1220 |
| M3-2 | | 49% α-MNT | 0.30 | 8 | 120 | 814 |

and α-methylnaphthalene did not react at the lean experimental conditions tested. Methylcyclohexane displayed unstable behaviour either producing runaway reaction or no reaction. For these reasons, the oxidative behavior of isocetane, methylcyclohexane, and methylnaphthalene was indirectly observed by blending them in binary mixtures with *n*-dodecane as a base fuel. The presence of *n*-dodecane accounted for the development of a radical pool large enough to initiate the oxidation of the other fuel, which would otherwise be unreactive at the tested conditions.

Considering pure *n*-dodecane, three CCD experiments were conducted at different conditions of equivalence ratio and the measured reactivity maps showing the CO formation as function of the temperature are presented in Fig. 3. Considering the CO production as a measure of the overall reactivity of the fuel, it is possible to note for all the experiments that the reaction rate is characterized by a monotonic increase as the temperature increases in the range 600–700 K. However, the overall reaction rate decreases as the temperature is further increased, specifically in the range 700–800 K. For these experiments no significant reactivity was observed between 800 and 900 K. The decrease in reactivity starting at approximately $700 \pm 5$ K clearly identifies the beginning of a negative temperature coefficient (NTC) regime. The NTC behavior has also been observed for different alkanes in several previous studies, and can be explained to occur through the competition between the low temperature chemistry, which is dominated by the peroxy chemistry, and the intermediate temperature chemistry, which is characterized by the $HO_2$ and $H_2O_2$ chemistry and termination reactions [4].

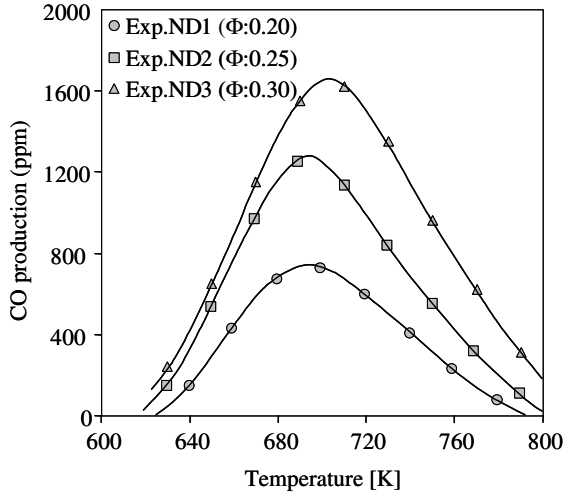


Fig. 3. *n*-Dodecane reactivity maps: effect of temperature and equivalence ratio on CO formation.

## 3. Kinetic modeling of reference components

As already mentioned, alkanes and cyclo-alkanes are the dominant components in liquid fuels. *n*-Dodecane and/or *n*-tetradecane are typical reference components for straight alkanes, while iso-octane and/or isocetane are used as model components for branched alkanes. In the cycloalkanes fraction, methylcyclohexane is commonly assumed as the reference molecule [9,14,15]. Due to their importance in gasoline oxidation, detailed kinetic modeling of normal and branched alkanes, typically *n*-heptane and iso-octane, has already been carried out and discussed for a number of years now, e.g., [16,17]. The definition of the primary reaction classes with their reference kinetic parameters easily allows for the application of our automatic generation methodology [18–20] to these heavier molecules.

A semi-detailed kinetic scheme, developed in earlier works for hydrocarbons up to *n*-dodecane, is extended here to larger species. The scheme uses a lumped description of the primary propagation reactions and primary intermediates for the large species and then treats the successive reactions of smaller species with a detailed kinetic scheme. This approach, together with an extensive use of structural analogies and similarities within the different reaction classes, easily allows extension of the kinetic scheme to new species. The lumped approach reduces the overall complexity of the resulting kinetic scheme both in terms of equivalent species and lumped or equivalent reactions. As discussed elsewhere [21], the 256 primary oxidation and propagation reactions of *n*-dodecane involve 72 new intermediate radicals and also 58 new intermediate components retaining the original *n*-C12 structure. For all these new components (6 *n*-dodecenes, 16 O-cyclicheters, 6 hydroperoxides and 30 keto-hydroperoxides) it is also necessary to include, in a detailed model, all the successive oxidation and decomposition reactions. It is easy to see that the dimensions of the problem will preclude the reliable extension and validation of the complete mechanism to heavy fuel mixtures. As shown in Fig. 4, the low and high temperature mechanism of *n*-dodecane oxidation is simply lumped with 4 intermediate radicals (alkyl radical: R12, peroxy radical: R12OO, hydroperoxy-alkyl radical: Q12OOH, alkyl hydroperoxy radical: OOQ12OOH) and 1 unstable molecule (kethohydroperoxyde: OQ12OOH) and it requires the description of the successive reactions of only 2 stable intermediate pseudo-species (oxygenated heterocycle: O-heter$_{12}$ and the conjugate alkene $C_{12}H_{24}$) retaining the original *n*-$C_{12}$ structure.

It is important to emphasize that this lumped model, despite its simplicity and extendibility, is able to catch not only the global reactivity of the system, but it also saves all the information about successive degradation steps, allowing the proper and accurate prediction

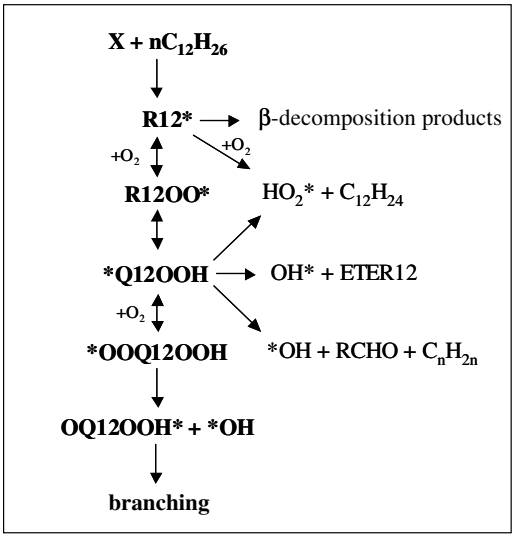


Fig. 4. Lumped kinetic scheme of *n*-dodecane oxidation.

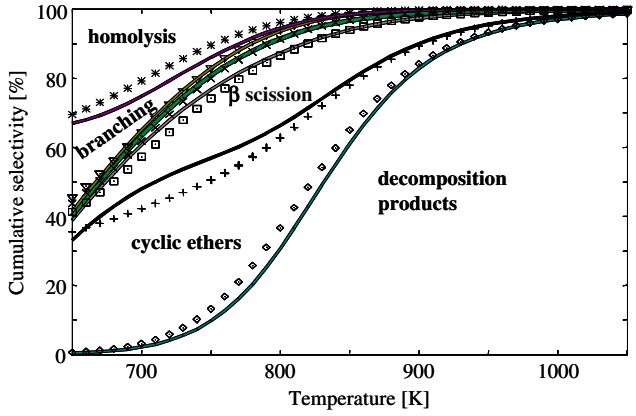


Fig. 5. Initial selectivity of primary products of isocetane oxidation at 1 atm. Comparison between detailed (marks) and lumped kinetics (lines).

of the formation of products and by-products, even those present in small amounts like pollutant PAH or $NO_x$.

This lumping technique can be conveniently explained referring to the primary oxidation reactions of isocetane (2,2,4,4,6,8,8-heptamethyl-nonane). By simply using the MAMOX+ program [19] it is easy to obtain the overall set of primary propagation reactions. These reactions involve 78 new intermediate radicals: 8 alkyl and 8 peroxy radicals, 31 alkyl hydroperoxyl and 31 peroxy alkylhydroperoxy radicals. The complexity of this detailed scheme becomes more evident when considering the necessity to describe the successive reactions of the large number of intermediate species. As a matter of facts, 9 alkenes with 15 C atoms are obtained by direct demethylation reactions of alkyl radicals and/or via decomposition reactions of the 31 alkyl hydroperoxy radicals. Similarly, 3 alkenes, 8 hydroperoxides, 17 cyclic ethers and 25 ketohydroperoxides retaining the initial carbon skeleton of the iso-cetane fuel are also formed. Therefore, it is very convenient to use a semi detailed approach, directly lumping in the initial stage the different isomers and considering in this way only one equivalent olefin, a cyclic-ether. The lumping rule, i.e. the definition of the isomer mixture, is based on the results of the detailed mechanism. The overall initial distribution of the different primary products is carried out on the basis of the primary reactions in a wide range of temperature and pressure conditions. The initial selectivity of the primary products (i.e. moles of product/100 mol decomposed at conversion approaching zero) is predicted by solving the linear system of continuity equations for all of the intermediate radicals (steady-state approximation). Fig. 5 shows the resulting selectivities of these primary products of the isocetane oxidation as a function of the temperature, and at 1 atm. The large selectivity of the cyclic-ether fraction in the intermediate temperature region is clearly evident. Following the approach already discussed in the analysis of iso-octane oxidation [22], it is convenient to distinguish two different lumped alkyl-hydroperoxy radicals ($Q_{16}OOH$ and $Q_{16}OOHt$) in order to take into account that the tertiary radicals can not follow the complete low temperature mechanism to form the ketohydroperoxides.

Table 2 reports the kinetic parameters of this lumped mechanism of isocetane. These parameters are estimated through an optimization process aimed to minimize the differences in the primary distribution products between the predictions of the lumped and detailed kinetic mechanisms in the whole investigated range of temperatures and pressures.

In a similar way, it is possible to develop the lumped mechanism for the low and high temperature oxidation of methyl-cyclohexane, as discussed elsewhere [23,24].

Finally, the primary propagation reactions of methylnaphthalene were already contained in the kinetic scheme and they were estimated on the basis of their similarity with the analogous reactions of naphthalene and toluene [25]. The resonantly stabilized radicals $C_{10}H_7CH_2$, mainly formed via H-abstraction reactions, play a significant role in methylnaphthalene reactivity and disappearance. This reaction set was studied in order to simulate the oxidation behavior of methylnaphthalene in the Princeton plug flow reactor [26] operating with 1100 ppm of fuel diluted in nitrogen at atmospheric pressure, $T = 1170$ K, and $\phi = 0.6$.

These subsets of lumped primary reactions of reference components of JP fuels were added to the overall kinetic scheme of hydrocarbon oxidation. The scheme also contains the successive reactions of intermediate species and it is then suitable for the analysis of all the CCD experiments.

Table 2
Isocetane primary lumped reactions

| | A | E |
|---|---|---|
| $RI_{16} \rightarrow 0.3375C_4H_8 + 0.5975C_8H_{16} + 0.065C_3H_6 + 0.18C_4H_9 + 0.125C_4H_9O_2 + 0.065C_5H_{11} + 0.13CH_3 + 0.5RI8 + 0.5C_8H_{16}$ | $1\times10^{14}$ | 29000 |
| $O_2 + RI_{16} \rightarrow HO_2 + C_{16}H_{32}$ | $0.25\times10^{9}$ | 3500 |
| $O_2 + RI_{16} \rightarrow RI_{16}OO$ | $2\times10^{9}$ | 0 |
| $RI_{16}OO \rightarrow RI_{16} + O_2$ | $0.63\times10^{14}$ | 30800 |
| $RI_{16}OO \rightarrow QOOHI_{16}I$ | $0.1\times10^{13}$ | 24000 |
| $QOOHI_{16}I \rightarrow RI_{16}OO$ | $0.12\times10^{13}$ | 20500 |
| $QOOHI_{16}I \rightarrow OH + 0.5CH_2O + 0.5C_4H_8O + 0.5C_3H_6 + 0.475C_4H_8 + 1.2C_8H_{16} + 0.25C_2H_4$ | $0.1\times10^{13}$ | 21500 |
| $QOOHI_{16}I \rightarrow cy\text{-}C_{16}H_{32}O + OH$ | $0.3\times10^{11}$ | 14500 |
| $QOOHI_{16}I \rightarrow HO_2 + C_{16}H_{32}$ | $0.15\times10^{12}$ | 21000 |
| $QOOHI_{16}I + O_2 \rightarrow OOQOOHI_{16}I$ | $2\times10^{9}$ | 0 |
| $OOQOOHI_{16}I \rightarrow QOOHI_{16}I + O_2$ | $0.2\times10^{14}$ | 30500 |
| $OOQOOHI_{16}I \rightarrow OQOOHI_{16} + OH$ | $0.2\times10^{11}$ | 24000 |
| $OQOOHI_{16} \rightarrow OH + 0.5C_3H_5O + 0.5C_2H_3O + 0.25CH_2O + 0.25C_2H_4O + 0.25C_3H_6O + 0.25C_4H_8O + 0.5625C_4H_8 + 0.25C_3H_6 + C_8H_{16}$ | $1\times10^{16}$ | 41000 |
| $RI_{16}OO \rightarrow QOOHI_{16}T$ | $0.13\times10^{13}$ | 26500 |
| $QOOHI_{16}T \rightarrow RI_{16}OO$ | $0.12\times10^{12}$ | 19500 |
| $QOOHI_{16}T \rightarrow OH + 0.5CH_2O + 0.5C_4H_8O + 0.5C_3H_6 + 0.475C_4H_8 + 1.2C_8H_{16} + 0.25C_2H_4$ | $0.2\times10^{13}$ | 22500 |
| $QOOHI_{16}T \rightarrow cy\text{-}C_8H_{16}O + OH + C_8H_{16}$ | $0.2\times10^{11}$ | 15000 |
| $QOOHI_{16}T \rightarrow HO_2 + C_{16}H_{32}$ | $0.15\times10^{12}$ | 21000 |
| $QOOHI_{16}T + O_2 \rightarrow OOQOOHI_{16}T$ | $2\times10^{9}$ | 0 |
| $OOQOOHI_{16}T \rightarrow QOOHI_{16}T + O_2$ | $0.63\times10^{14}$ | 30000 |
| $OOQOOHI_{16}T \rightarrow HO_2 + C_4H_8O + 0.25\ C_4H_8 + C_3H_6O + C_8H_{16}$ | $0.25\times10^{10}$ | 22500 |
| $OOQOOHI_{16}T \rightarrow OH + CH_2O + C_3H_6O + 0.79C_4H_8O + 0.21C_3H_6O + 0.0525C_4H_8 + C_8H_{16}$ | $0.15\times10^{13}$ | 27500 |

Units: l, mol, s, cal.

## 4. Comparisons between model predictions and experimental measurements

Fig. 6 shows a comparison between the experimental measurements of *n*-dodecane oxidation reported in Fig. 3, and the initial model predictions. Simulation results were obtained by considering, as reference temperature, the outlet temperature from an adiabatic plug flow reactor with a residence time of 120 ms. Only the runs ND-1 and ND-3 were considered and both the experiments confirm the capability of the model to properly predicts the location and the values of the maximum CO formation. In order to better explain the meaning of these low temperature reactivity maps, Fig. 2 shows the predicted behavior of CO and $CO_2$ formation also in the high temperature conditions for the ND-1 system. The maximum CO formation at low temperatures corresponds to about 6% of the carbon fed.

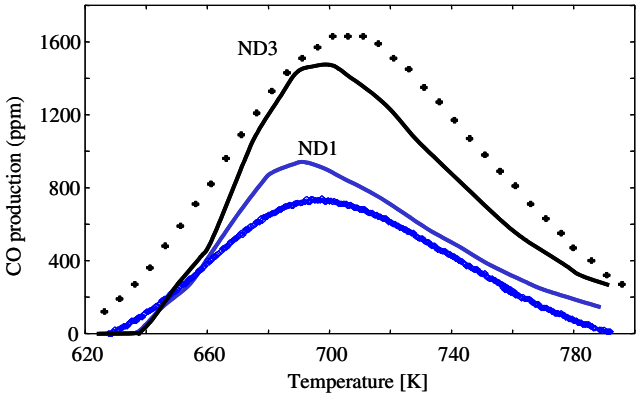


Fig. 6. CO production vs. reactor temperature for *n*-dodecane oxidation (ND1 and ND3). Comparison of experimental measures (points) vs. simulation results (lines).

As reported in Table 1, in order to study the synergistic and antagonistic effects of mixtures, three sets of CCD experiments were conducted with addition of isocetane, methylcyclohexane and methylnaphthalene in *n*-dodecane. Conditions were selected to directly compare the reactivity of these mixtures with that of neat *n*-dodecane.

The mixture M1 was constituted of 40% of *n*-dodecane and 60% of isocetane. Two CCD experiments were conducted at different conditions of fuel molar fraction, keeping the other parameters constant. Fig. 7 shows the resulting reactivity maps for the M1-1 and M1-2 experiments. It can be observed that the interaction between the two fuels is not linear, that is the mixture was more reactive than a linear blend of the two components. In fact, simply considering the richer experimental conditions of exp. M1-1, pure isocetane would not even react at these conditions, while 350 ppm of *n*-dodecane (i.e., 40% of the fuel molar fraction for exp. M1-1) would produce a maximum CO of approximately 315 ppm, based on the interpolation of the pure *n*-dodecane experimental results.

The second binary mixture oxidized, M2, contains 37% of *n*-dodecane and 63% of methylcyclohexane. Two CCD experiments were conducted (see Table 1) and the

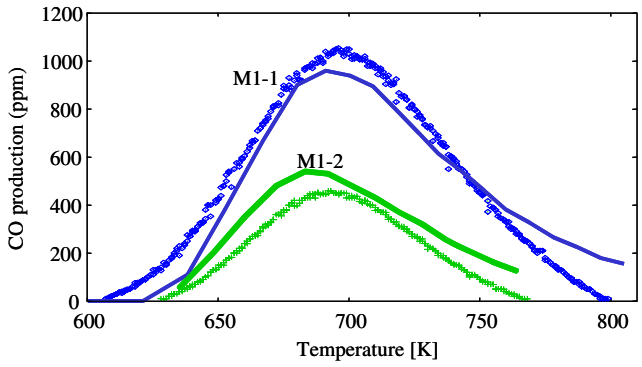


Fig. 7. CO production vs. reactor temperature for *n*-dodecane and isocetane mixture oxidation (series M1-1 and M1-2). Comparison of experimental measures (points) vs. simulation results (lines).

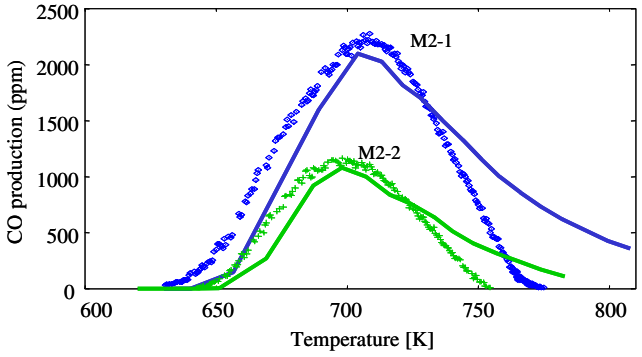


Fig. 8. CO production vs. reactor temperature for *n*-dodecane and methylcyclohexane mixture oxidation (series M2-1 and M2-2). Comparison of experimental measures (points) vs. simulation results (lines).

reactivity maps are shown in Fig. 8. Also in this case, and for both the experiments, the interactions between the two fuels resulted in a synergistic effect. Simply considering the richer experimental conditions of exp. M2-1, pure methylcyclohexane would not even react, while 560 ppm of *n*-dodecane (i.e., 37% of the fuel molar fraction for exp. M2-1) would produce a maximum CO of approximately 1270 ppm (exp. ND-2).

Model predictions agree well with the experimental measurements in terms of initial reactivity as well as in terms of the values and locations of maximum CO. The model slightly over predicts the residual reactivity of the system at intermediate temperatures.

The third binary mixture, M3, contains 51% of *n*-dodecane and 49% of α-methylnaphthalene. Fig. 9 shows the maps of two CCD experiments and the comparisons with the theoretical results. The kinetic model only partially predicts the decrease in CO production for mixture M3 with respect to pure *n*-dodecane. As a matter of fact, experimental measurements show that the interaction between the aromatic and the alkane components of the mixture produces an inhibiting effect. In fact, comparing the CO production for exp. M3-1 ($CO_{peak} = 1030$, *n*-dodecane molar fraction = 630 ppm) with that of pure *n*-dodecane (exp. ND-3, $CO_{peak} = 1660$, *n*-dodecane molar fraction = 680 ppm), it is clear that the addition of the aromatic component reduced the reactivity over that of pure *n*-dodecane. This result experimentally confirms and theoretically explains previous studies of Wilk and coworkers, showing that the addition of aromatics has an inhibiting effect on the chemistry of alkanes [13]. From the kinetic point of view, a sensitivity analysis on this system reveals the importance of the oxygen interactions with the stable aromatic radicals and confirms the need to introduce and to use in the overall kinetic scheme two different isomeric radicals $C_{11}H_9$, respectively with phenyl and benzyl characteristics [11]. Moreover the deviations observed in Fig. 9, seem also to indicate the need to better investigate the possible low temperature interactions of the resonantly stabilized radical $C_{10}H_7CH_2$ with oxygen.

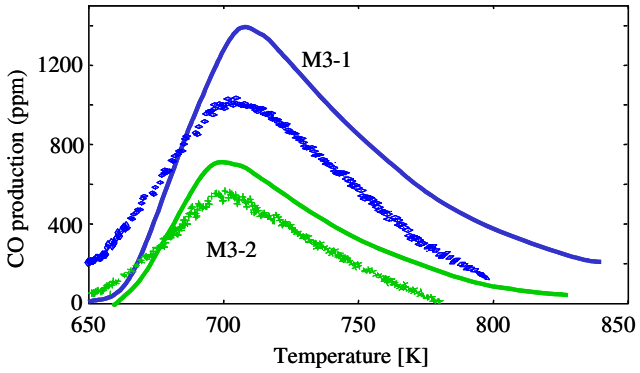


Fig. 9. CO production vs. reactor temperature for *n*-dodecane and methylnaphthalene mixture oxidation (series M3-1 and M3-2). Comparison of experimental measures (points) vs. simulation results (lines).

## 5. Conclusions

This work presents the comparisons between experimental data and fully predictive theoretical computations for the low temperature oxidation of mixtures of reference components of JP-8. The CCD experimental measurements were carried out in the PFR of Drexel University. The semi-detailed kinetic mechanism was developed at Politecnico di Milano. The preliminary results and the quite good match observed indicate the reliability of the model, which was not tuned based on the measurements. Nevertheless some further activity is required to cover uncertainties and deviations. Particularly the low temperatures behavior of the aromatic compounds has to be better described. As a matter of fact, some deviations in the comparison with the experimental measurements could be attributed to the

adopted lumping approach. Therefore, this aspect requires further study and perhaps experimental confirmation.

Finally, it is noted that the fruitful results coming from this joint activity combining both experimental and modeling perspectives allows development of an understanding of the detailed chemistry of hydrocarbon oxidation. Needless to say, such collaborations should be encouraged in the future.

## Acknowledgements

The authors wish to thank Prof. Adel Sarofim for the helpful suggestions and they also acknowledge the useful work of Alba Corradini and Marina Riccio. The experimental part of this work has been funded by the US Army Research Office, Contract No. DAAG 55-98-1-0286, and by the National Science Foundation, Contract No. CTS-9910563. The kinetic modeling work was carried out with MURST-PRIN and ENEA 2001 financial support.

## References

[1] N.P. Cernansky, R.M. Green, W.J. Pitz, C.K. Westbrook, Chemistry of fuel oxidation proceedings end gas autoignition, Combust. Sci. Technol. 50 (1986) 3–15.
[2] T.A. Litzinger, A review of experimental studies of knock chemistry in engines, Prog. Energy Combust. Sci. 16 (3) (1990) 155–167.
[3] F.L. Dryer, The phenomenology of modeling combustion chemistry, in: W. Bartok, A.F. Sarofim (Eds.), Fossil Fuel Combustion: A Source Book, John Wiley and Sons, New York, 1991.
[4] M.J. Pilling, Comprehensive Chemical Kinetics 35: Low-Temperature Combustion and Autoignition, Elsevier, Amsterdam, 1997.
[5] T. Edwards, USAF supercritical hydrocarbon fuels interests, AIAA Paper No. 93-0807, 1993.
[6] R.P. Lindstedt, L.Q. Maurice, Detailed chemical kinetic model for aviation fuels, J. Propulsion Power 16 (2) (2000) 187–195.
[7] C.J. Montgomery, S.M. Cannon, M.A. Mawid, B. Sekar, Reduced chemical kinetic mechanisms for JP-8 combustion, 40th AIAA Aerospace Sciences Meeting and Exhibit, Reno, Nevada, January 2002, Paper No. 2002-0336.
[8] T. Edwards, Real kerosene aviation and rocket fuels: composition and surrogates, Fall Technical Meeting Eastern State Section of the Combustion Institute, Hilton Head, South Carolina, December 2001, Paper No. 2001-61.
[9] A. Agosta, Development of a chemical surrogate for JP-8 aviation fuel using a pressurized flow reactor, M.S. Thesis, Drexel University, Philadelphia PA, 2002.
[10] L.Q. Maurice, H. Lander, T. Edwards, W.E. Harrison III, Advanced aviation fuels: a look ahead via a historical perspective, Fuel 80 (2001) 747–756.
[11] S. Granata, T. Faravelli, E. Ranzi, N. Olten, S. Senkan, Kinetic modeling of counter-flow diffusion flames of butadiene and mixing effect, Combust. Flame 131 (3) (2002) 267–278.
[12] D.N. Koert, N.P. Cernansky, A flow reactor for the study of homogeneous gas phase oxidation of hydrocarbons at pressures up to 20 atm, Meas. Sci. Technol. 3 (6) (1992) 607–613.
[13] R.D. Wilk, D.N. Koert, N.P. Cernansky, Low temperature carbon monoxide formation as a means of assessing the autoignition tendency of hydrocarbons and hydrocarbon blends, Energy Fuels 3 (3) (1989) 292–298.
[14] T. Edwards, L.Q. Maurice, Surrogate mixtures to represent complex aviation and rocket fuels, J. Propulsion Power 17 (2) (2001) 461–466.
[15] A. Violi, S. Yan, E.G. Eddings, A.F. Sarofim, S. Granata, T. Faravelli, E. Ranzi, Experimental formulation and kinetic model for JP-8 surrogate mixtures, Combust. Sci. Techn. 174 (11–12) (2002) 399–417.
[16] R.T. Pollard, in: C.J. Bamford, C.F.H. Tipper, R.G. Compton (Eds.), Comprehensive Chemical Kinetics, Elsevier, Amsterdam, 1977, p. 249.
[17] C. Morley, A fundamentally based correlation between alkane structure and octane number, Combust. Sci. Tech. 55 (1987) 115–123.
[18] G.M. Come, V. Warth, P.A. Glaude, R. Fournet, F. Battin Leclerc, G. Scacchi, Proc. Comb. Inst. 26 (1996) 755.
[19] E. Ranzi, T. Faravelli, P. Gaffuri, E. Garavaglia, A. Goldaniga, Primary pyrolysis and oxidation reactions of linear and branched alkanes, Ind. Eng. Chem. Res. 36 (8) (1997) 3336–3344.
[20] G. Bikas, N. Peters, Kinetic modeling of *n*-decane combustion and autoignition, Combust. Flame 126 (2001) 1456–1475.
[21] E. Ranzi, M. Dente, G. Bozzano, A. Goldaniga, T. Faravelli, Lumping procedures in detailed kinetic modeling of gasification, pyrolysis, partial oxidation and combustion of hydrocarbon mixtures, Progr. Energy Comb. Science 27 (2001) 99–139.
[22] E. Ranzi, T. Faravelli, P. Gaffuri, A. Sogaro, A. D'Anna, A. Ciajolo, A wide range modeling study of iso-octane oxidation, Combust. Flame 108 (1997) 24–42.
[23] A. Corradini, M. Riccio, Cinetica dettagliata di combustibili liquidi, Thesis, Politecnico di Milano, 2002.
[24] S. Granata, T. Faravelli, E. Ranzi, A wide range kinetic modeling study of pyrolysis and combustion of naphthenes, Combust. Flame 132 (3) (2003) 533–544.
[25] A. Goldaniga, L. Zappella, T. Faravelli, M. Dente, E. Ranzi, 'Reaction classes and lumping criteria for the extension of detailed kinetic schemes to heavy PAH' Italian Section of the Combustion Institute Ischia May 2000.
[26] C.R. Shaddix, K. Brezinsky, I. Glassman, Oxidation of 1-methylnaphthalene, Proc. Comb. Inst. 24 (1992) 683–690.